(Preprint) AAS 19-431

DIFFERENTIAL LIFT AND DRAG CONSTELLATION CONTROL USING TRIMMED ATTITUDE

Andrew Harris* **and Hanspeter Schaub†**

Spacecraft operating in Low Earth Orbit can leverage atmospheric forces to reduce fuel consumption and improve robustness to hardware failure. This work aims to extend prior work in differential-drag formation flight to the constellation domain through the use of linearized relative orbital elements. A gas-surface interaction model is evaluated for multiple possible surface material properties, demonstrating the potential feasibility of lift forces for actuating specially-designed spacecraft. Small variations to attitude about a reference attitude–referred to as "trimmed attitude" in this work–are considered as the control input, allowing for the construction of a system that is affine in control. A Lyapunov-based control strategy is derived and demonstrated in simulation to validate the lift sensitivity matrix.

INTRODUCTION

The high mission cost and risk of propellant-based maneuvers has long motivated astrodynamicists to look to the space environment as a source of actuating forces and torques. For many proposed Low Earth Orbit missions (LEO), forces from spacecraft-atmosphere interactions are a dominant disturbance force;[1] in the context of coordinated multi-spacecraft missions ("constellation" or "formation"–based missions), gains from reduced fuel consumption or increased robustness to failure are potentially realized across dozens or hundreds of spacecraft, providing further motivation. Prior work has shown that atmospheric "drag" forces can be used to conduct in-plane orbit control with respect to another drag-perturbed orbit.[2] For spacecraft with fixed, non-uniform geometries, atmospheric forces directly couple attitude and orbital motion.[3] This work aims to extend prior studies by considering additional forces from specular reflection of atmospheric particles (referred to as "atmospheric lift") to control out-of-plane differential orbital elements.

Many prior studies in atmospheric spacecraft control have focused on the use of atmospheric "drag" forces to control spacecraft in the field of differential-drag formation flight. Within this area, studies can be further grouped into flap-driven continuous control[4][5][6] (which assumes the use of deployable drag panels or areas which can vary continuously as an actuator), bang-bang attitude control[7][2] (which switches between discrete attitude states to produce relative accelerations), and continuous attitude-driven differential drag control.[8] While each approach has merits and drawbacks, drag forces are constrained to act within the orbital plane, preventing their application towards out-of-plane maneuvers. By contrast, the orientation-dependent nature of lift forces from specular reflection allows them to act outside the orbit plane, potentially providing a means of conducting expensive plane-change maneuvers. Models of gas-surface interactions for spacecraft, such

*Research Assistant, Smead Department of Aerospace Engineering Sciences, Graduate Student, University of Colorado Boulder, Boulder, CO, 80309 USA.

†Glenn L. Murphy Chair of Engineering, Smead Department of Aerospace Engineering Sciences, University of Colorado,

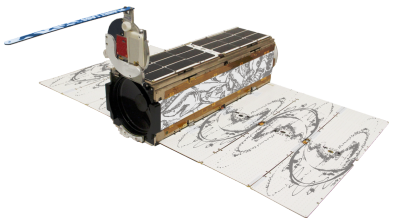

Figure 1. A PlanetLabs Dove spacecraft demonstrating non-uniform geometry

as the one presented by Bird[9] and refined for astrodynamics use by Pilinski,[10] predict the presence of so-called "lift" forces due to specular particle reflection off polished surfaces. With suitable spacecraft geometries, these "lift" forces could be directed out of the orbital plane to counteract the affects of other out-of-plane disturbance forces, or provide a means of conducting expensive plane-change maneuvers. Prior work in this area showed local formation controllability under the assumption of unlimited atmospheric lift, without explicitly including lift feasibility in their control design.[7] Other work in aero-assisted maneuvering focuses on conducting plane-change maneuvers during aerobraking or aerocapture passes[11],[12] however, doing so requires specialized spacecraft design to both generate substantial amounts of lift at high speed and survive the sustained heat of aerobraking passes. This work will expand upon prior studies in lift-based orbit control by considering gas-surface interaction models in its analysis of system controllability, thereby implicitly examining the feasibility of lift-based orbit control directly.

An outline of this work is presented for the benefit of the reader. First, a model of attitude-dependent lift and drag is presented for spacecraft, with a brief discussion on reasonable values of drag and lift coefficients for current and future spacecraft. Next, the affects of spacecraft lift and drag on Keplerian orbital elements are considered using Gauss' Variational Equations. These models are then linearized about an equilibrium configuration representing a desired end-state or rendezvous target to determine conditions for linear controllability. Finally, these approaches are validated in simulation by using spacecraft attitude to conduct a plane-change maneuver using only atmospheric forces.

PROBLEM STATEMENT

Coordinate Frame Definitions

Before addressing the system model, it is important to define the reference frames which define the problem. First is the planet-centered inertial frame N, which is taken as the global origin of the system:

$$N = \{\mathbf{0}, \hat{\boldsymbol{n}}_1, \hat{\boldsymbol{n}}_2, \hat{\boldsymbol{n}}_3\} \tag{1}$$

Next is the Hill frame H, which is centered on the spacecraft at a given position $\boldsymbol{r}_{H/N}$ in orbit and consists of the following unit vectors:

$$H = \{\boldsymbol{r}_{H/N}, \hat{\boldsymbol{h}}_r, \hat{\boldsymbol{h}}_\theta, \hat{\boldsymbol{h}}_h\} \tag{2}$$

where $\boldsymbol{r}_{H/N}$ is the position vector of the spacecraft with respect to the center of the N frame and

431 UCB, Colorado Center for Astrodynamics Research, Boulder, CO 80309-0431. AAS Fellow.

the unit vectors are defined as follows:

$$\hat{\boldsymbol{h}}_r = \frac{\boldsymbol{r}_{H/N}}{\|\boldsymbol{r}_{H/N}\|} \tag{3}$$

$$\hat{\boldsymbol{h}}_h = \frac{\boldsymbol{r}_{H/N} \times \dot{\boldsymbol{r}}_{H/N}}{\|\boldsymbol{r}_{H/N}\|\|\dot{\boldsymbol{r}}_{H/N}\|} \tag{4}$$

$$\hat{\boldsymbol{h}}_\theta = \hat{\boldsymbol{h}}_h \times \hat{\boldsymbol{h}}_r \tag{5}$$

The direction cosines matrix that maps vectors from H to N, denoted as $[HN]$, is expressed by:

$$[HN] = \begin{bmatrix} \hat{\boldsymbol{h}}_r^T \\ \hat{\boldsymbol{h}}_\theta^T \\ \hat{\boldsymbol{h}}_h^T \end{bmatrix} \tag{6}$$

The angular velocity of H with respect to N is given by the spacecraft's mean motion n, which forms the angular velocity vector ${}^{\mathcal{N}}\boldsymbol{\omega}_{H/N} = \dot{f}\hat{\boldsymbol{h}}_h$, where $\dot{f}$ is the orbit true anomaly rate. For circular orbits, the true anomaly rate is equal to the mean anomaly rate n.

Finally, the spacecraft body frame B is defined, which is aligned with the spacecraft's principal inertia frame and written as the following:

$$B = \{\boldsymbol{r}_{H/N}, \hat{\boldsymbol{b}}_1, \hat{\boldsymbol{b}}_2, \hat{\boldsymbol{b}}_3\} \tag{7}$$

The angular velocity vector between the body and inertial frames is given generally as:

$${}^{\mathcal{B}}\boldsymbol{\omega}_{B/N} = \begin{bmatrix} \omega_1 & \omega_2 & \omega_3 \end{bmatrix}^T \tag{8}$$

Nonlinear Dynamics

With the system reference frames established, the dynamics that underly this work are next defined. A spacecraft experiencing spherical two-body gravity with other perturbation accelerations obeys the following equations of motion:[1]

$$\ddot{\boldsymbol{r}} = -\frac{\mu}{r^3}\boldsymbol{r} + \boldsymbol{a}_p \tag{9}$$

where $\boldsymbol{r}$ is the inertial spacecraft position vector, μ is the planet's gravitational parameter, and $\boldsymbol{a}_p$ is the inertial perturbing acceleration vector. For the purposes of this analysis, the perturbing accelerations are assumed to be purely a function of the spacecraft's interactions with the atmosphere.

The objective of this work is to maneuver a spacecraft in one orbit to a desired target orbit; as such, the existence of two orbits naturally lends itself to the use of a relative motion formulation. The controlled expression is therefore the "orbit error" between the desired and target orbits:

$$\Delta\boldsymbol{oe} = \boldsymbol{oe} - \boldsymbol{oe}_d \tag{10}$$

where $\boldsymbol{oe}$ represents a general six-element vector of orbital elements, and $\boldsymbol{oe}_d$ represents the target orbital element vector. For the purposes of this work, Linearized Relative Orbital Elements

(LROEs) are used as a physically interpretable, non-singular relative motion parameterization.[13] These elements are defined in terms of the rectilinear Hill-frame states for reference here:

$$A_1 = -\frac{(3nx + 2\dot{y})\cos(nt) + \dot{x}\sin(nt)}{n} \tag{11}$$

$$A_2 = \frac{(3nx + 2\dot{y})\sin(nt) - \dot{x}\cos(nt)}{n} \tag{12}$$

$$x_{\text{off}} = 4x + \frac{2\dot{y}}{n} \tag{13}$$

$$y_{\text{off}} = -2\frac{\dot{x}}{n} + y + (6nx + 3\dot{y})t \tag{14}$$

$$B_1 = z\cos(nt) - \frac{\dot{z}\sin(nt)}{n} \tag{15}$$

$$B_2 = -z\sin(nt) - \frac{\dot{z}\cos(nt)}{n} \tag{16}$$

Each of these elements represents a geometric component of the relative motion; the size and shape of the in-plane relative orbit (A_1 and A_2), the center of the relative orbit in the orbital plane (x_{off} and y_{off}), and the shape of the out-of-plane component of the relative orbit (B_1 and B_2). Under Keplerian dynamics, these orbital elements are constant and given in units of distance. The effect of a disturbing Hill-frame acceleration on these elements can be computed directly by using the LROE sensitivity matrix:[13]

$$[B_{\text{LROE}}] = \frac{1}{n}\begin{bmatrix} -\sin(nt) & -2\cos(nt) & 0 \\ -\cos(nt) & 2\sin(nt) & 0 \\ 0 & 2 & 0 \\ -2 & 3nt & 0 \\ 0 & 0 & -\sin(nt) \\ 0 & 0 & -\cos(nt) \end{bmatrix} \tag{17}$$

Notably, these sensitivities are time-dependent, and include a component that grows secularly with time.

Aerodynamics Model

Foundational to the success of this approach is the feasibility of using lift under an assumed gas-surface interaction model. Gas surface interactions are a relatively poorly understood phenomena for spacecraft, as few samples of space-weathered material have been returned to earth and the conditions under which adsorption occurs are difficult to replicate on the ground.

One commonly-used analytical model for spacecraft applications is presented by Sentman[9] and refined for astrodynamics use by Pilinksi.[10] It provides the coefficients of lift and drag for the i^th flat plate exposed on one side to a Maxwellian flow:

$$C_{D,i} = \frac{2}{s\sqrt{\pi}}\exp(-s^2\sin^2(\theta_{\text{in}})) + \frac{\sin(\theta_{\text{in}})}{s^2}(1 + 2s^2)\text{erf}(s\sin(\theta_{\text{in}})) + \frac{\sqrt{\pi}}{s}\sin^2(\theta_{\text{in}})\sqrt{T_{k,\text{out}}/T_a} \tag{18}$$

$$C_{L,i} = \frac{\cos(\theta_{\text{in}})}{s^2}\text{erf}(s\cos(\theta_{\text{in}})) + \frac{1}{s}\sqrt{\pi}\cos(\theta_{\text{in}})\sin(\theta_{\text{in}})\sqrt{T_{k,\text{out}}/T_a} \tag{19}$$

where $s = |\boldsymbol{v}|\sqrt{m/(2k_BT_a)}$, k_B is the Boltzman constant, T_a represents the bulk ambient particle velocity, $T_{k,\text{out}}$ represents the reflected kinetic temperature of particles at the surface, erf() represents

the error function, and θ_{in} represents the principle rotation angle between the spacecraft-atmosphere velocity vector and the surface normal direction. Both the lift and drag coefficients are functions of both the spacecraft attitude (which governs θ_{in}) and surface material properties, which affect T_k through the accommodation coefficient α:

$$T_{k,\text{out}} = \frac{m}{3k_B}|\boldsymbol{v}|^2(1-\alpha) + \alpha T_w \tag{20}$$

where T_w is the temperature of the facet surface. The lift and drag coefficients produced by these expressions are related to the lift and drag accelerations acting on a spacecraft modeled as a single flat plate by:

$$\mathbf{a}_D = -\frac{1}{2m}\sum_{i=1}^{N_p}(C_{D,i}A_{p,i})P|v|\mathbf{v} \tag{21}$$

$$\mathbf{a}_L = -\frac{1}{2m}\sum_{i=1}^{N_p}(C_{L,i}A_{p,i})P|v|(\hat{\boldsymbol{v}} \times \hat{\boldsymbol{n}} \times \hat{\boldsymbol{v}}) \tag{22}$$

where $A_{p,i}$ is the projected area of an individual facet into the flow, N_p is the number of exposed facets, v is the spacecraft's velocity, P is the local neutral atmospheric density, and $\hat{\boldsymbol{n}}$ is the normal vector of a single facet. The projected area is dependent on the dot product of the surface normal and the atmosphere-relative velocity vector:

$$A_p = A_i({}^{\mathcal{B}}\hat{\boldsymbol{n}}^T[BN(\boldsymbol{\sigma}_r)]^{\mathcal{N}}\hat{\boldsymbol{v}}) \tag{23}$$

From these expressions, it is apparent that drag accelerations are strictly in opposition to the spacecraft velocity vector, and are therefore constrained to act within the orbit frame. The direction of so-called "lift" forces, on the other hand, is dependent on the orientation between the spacecraft's surfaces and the flow. This implies that lift forces are not constrained by the orbit plane, and can therefore change the plane of a given spacecraft.

Lift Coefficient Feasibility

The magnitude of lift forces for spacecraft are constrained by the accommodation coefficients of their flow-exposed surfaces, which affect the value of $T_{k,\text{out}}$. Many empirical studies of spacecraft accommodation coefficients place the value at or close to 1, representing complete surface accommodation of incoming particles. As a result, lift forces are often neglected completely during orbital perturbations studies, as the resulting lift coefficients and forces are small. These empirical accommodation and therefore lift coefficients have been used to drive prior studies in lift-based control, as done by 7.

These works leave open the possibility of exotic materials to reduce accommodation coefficients. Prior studies have indicated that, for materials such as gold, nickel, nad reaction-cured glass, surface accommodation coefficients as low as 0.3 are possible under interaction with atomic oxygen at orbital velocities.[14] If these coefficients can be maintained on-orbit, the possibility of using lift-based control becomes far more feasible.

Figure 2 shows the possible range of lift and drag coefficients for a flat plate with an accommodation coefficients of 0.3 versus 0.9, using the additional parameters specified in Table 1. As is expected for the decomposition of specular and diffuse reflection into a lift-drag coordinate frame,

Table 1. Assumed spacecraft geometric and material parameters.

Parameter	Value
A_{ref}	6628.137 km
$\lvert\boldsymbol{v}\rvert$	0
T_{surf}	293 K
ρ	2.5 $\times 10^{-7}$ $\frac{\text{kg}}{\text{m}^3}$
T_{atmo}	300 K
m	8.0

lift forces approach zero as the facet attitude approaches the flow-on zero attitude where drag is maximized.

For the purposes of this analysis, it is assumed that one facet of a spacecraft has been coated with a low-accommodation coefficient material ($\alpha = 0.3$) whose performance is well understood and is static with respect to time.

General Atmospheric Force Vector Derivation

Many prior studies involving the effects of atmospheric forces for orbit control have used linearized Cartesian coordinates[15] to represent the position and velocity of a given spacecraft; however, these coordinates lack physical interpretability. Differential orbital elements are another commonly-used framework to represent large relative separations. Other studies which have leveraged the classical Keplerian elements, such as Reference 16, encounter singularities when zero eccentricity or inclination target orbits are considered. When considering drag effects as a circularizing force, these drawbacks are significant.

Instead, a nonsingular relative orbit parameterization is sought. Most relative orbital element strategies depend implicitly on the variational equations for an orbital element set, and therefore use Hill-frame acceleration vectors, defined here using the vector $\boldsymbol{a} = \begin{bmatrix} a_r & a_\theta & a_h \end{bmatrix}^T$ as their control input. Here, the differential aerodynamic acceleration vector is derived in Hill-frame components.

To simplify the application of lift and drag, an intermediate velocity frame is defined based on a spacecraft's inertial velocity vector as

$$\hat{\imath}_{\mathbf{v}} = \frac{\boldsymbol{v}}{||\boldsymbol{v}||} \tag{24}$$

$$\hat{\mathbf{i}}_{\mathbf{h}} = \frac{\boldsymbol{r} \times \boldsymbol{v}}{||\boldsymbol{r} \times \boldsymbol{v}||} \tag{25}$$

$$\hat{\mathbf{i}}_{\mathbf{n}} = \hat{\mathbf{i}}_{\mathbf{v}} \times \hat{\mathbf{i}}_{\mathbf{h}} \tag{26}$$

Comparing this to the classic Hill frame, this velocity-derived frame is simply a rotation about the $\hat{\mathbf{i}}_{\mathbf{n}}$ axis:

$$\begin{bmatrix} \hat{\imath}_{\mathbf{n}} \\ \hat{\imath}_{\mathbf{v}} \\ \hat{\imath}_{\mathbf{h}} \end{bmatrix} = \frac{h}{pv} \begin{bmatrix} p/r & -e\sin(f) & 0 \\ e\sin(f) & p/r & 0 \\ 0 & 0 & 1 \end{bmatrix} \begin{bmatrix} \hat{\imath}_{\mathbf{r}} \\ \hat{\imath}_{\theta} \\ \hat{\imath}_{\mathbf{h}} \end{bmatrix} \tag{27}$$

Because both rotate with the same velocity relative to the inertial frame ($\omega_{ON} = \begin{bmatrix} 0 & 0 & \dot{f} \end{bmatrix}$), the acceleration components can be expressed using the transpose of $[VO]$:

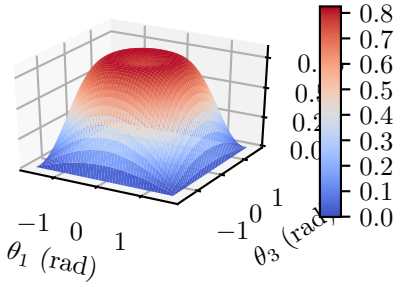

(a) Drag Coefficient Sweep, α=0.3

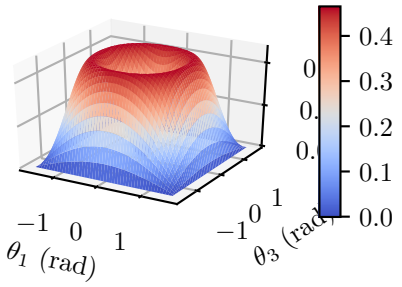

(b) Lift Coefficient Sweep, α=0.3

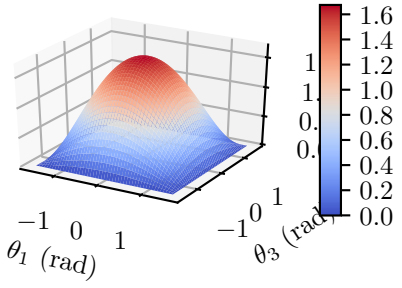

(c) Drag Coefficient Sweep, α=0.9

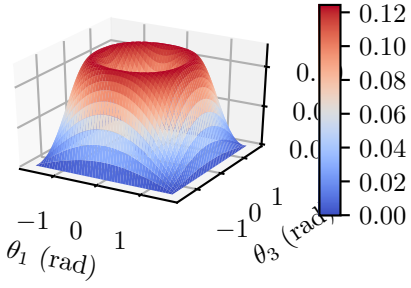

(d) Lift Coefficient Sweep, α=0.9

Figure 2. Lift and drag coefficients for a flat plate under the Sentman quasi-specular model versus flow-relative pitch (θ_1) and yaw (θ_2) rotations.

$$\begin{bmatrix} \hat{\imath}_{\mathbf{r}} \\ \hat{\imath}_{\theta} \\ \hat{\imath}_{\mathbf{h}} \end{bmatrix} = \frac{h}{pv} \begin{bmatrix} p/r & e\sin(f) & 0 \\ -e\sin(f) & p/r & 0 \\ 0 & 0 & 1 \end{bmatrix} \tag{28}$$

With this in hand, the drag-driven equations of motion are straightforward to derive, as the drag accelerations act only along the velocity axis. Lift, on the other hand, requires the incorporation of spacecraft geometry due to its dependence on specular reflection. Per Pilinski,[10] the lift direction is

$$\mathbf{i}_{\mathbf{L}} = (\hat{\mathbf{v}} \times \hat{\mathbf{n}}) \times \hat{\mathbf{v}} \tag{29}$$

The surface normal is taken with general components in the velocity frame:

$$^{\mathcal{V}}\boldsymbol{v} = \begin{bmatrix} 0 & v & 0 \end{bmatrix} \tag{30}$$

$$^{\mathcal{V}}\hat{\mathbf{n}} = \begin{bmatrix} n_1 & n_2 & n_3 \end{bmatrix} \tag{31}$$

In the velocity frame, this is equivalent to:

$$^{\mathcal{V}}\hat{\mathbf{i}}_{\mathbf{L}} = \begin{bmatrix} n_1 \\ 0 \\ n_3 \end{bmatrix} \tag{32}$$

This is rotated into the Orbit frame by Equation 28:

$$^{\mathcal{O}}\hat{\mathbf{n}} = \begin{bmatrix} \frac{hn_1}{rv} \\ -\frac{ehn_1 \sin(f)}{pv} \\ \frac{hn_3}{pv} \end{bmatrix} \tag{33}$$

This allows for the expression of the lift vector in terms of the Hill-frame normal vector:

$$^{\mathcal{O}}\boldsymbol{a}_L = \begin{bmatrix} Q_L(\frac{hn_1}{rv}) - Q_D e \sin(f) \\ Q_L(-\frac{ehn_1 \sin(f)}{pv}) - Q_D \frac{p}{r} \\ Q_L \frac{hn_3}{pv} \end{bmatrix} \tag{34}$$

where Q_L is the magnitude of the lift force given by

$$Q_L = \frac{-1}{2m} C_L A_{proj} P |v|^2 \tag{35}$$

with the analogous drag force and direction given by

$$Q_D = \frac{-1}{2m} C_D A_{proj} |v|^2 \rho, \; ^{\mathcal{V}}\boldsymbol{a}_D = \begin{bmatrix} 0 & Q_D & 0 \end{bmatrix} \tag{36}$$

Because the lift acceleration can have components in each direction depending on the orientation of the plate normal vector, it affords considerably more opportunities for atmospheric interaction to affect the trajectory of a spacecraft.

Using these expressions, it is apparent that the addition of atmospheric lift allows for spacecraft-atmosphere interactions to create accelerations in all directions, as opposed to the in-plane only accelerations afforded by drag alone. To examine the sensitivity of the atmospheric acceleration vector to attitude variation, the expression of the surface normal components in the orbit frame is examined in terms of the spacecraft attitude:

$$^{\mathcal{O}}\begin{bmatrix} n_1 \\ n_2 \\ n_3 \end{bmatrix} = [OB(\boldsymbol{\sigma}_{OB})]^{\mathcal{B}}\hat{\boldsymbol{n}} \tag{37}$$

Under the assumption of small MRPs, the attitude dependence becomes

$$^{\mathcal{O}}\begin{bmatrix} n_1 \\ n_2 \\ n_3 \end{bmatrix} = ([I] - 4[\boldsymbol{\sigma}_p \times])^{\mathcal{B}}\hat{\boldsymbol{n}} \tag{38}$$

leading to the substitutions

$$n_1 = b_1 + 4\sigma_3 b_2 - 4\sigma_2 b_3 \tag{39}$$

$$n_2 = b_2 - 4\sigma_3 b_1 + 4\sigma_1 b_3 \tag{40}$$

$$n_3 = b_3 + 4\sigma_2 b_1 - 4\sigma_1 b_2 \tag{41}$$

$$^{\mathcal{O}}\boldsymbol{a}_L = \begin{bmatrix} Q_L(\frac{h(b_1+4\sigma_3 b_2 - 4\sigma_2 b_3)}{rv}) - Q_D e \sin(f) \\ Q_L(-\frac{eh(b_1+4\sigma_3 b_2 - 4\sigma_2 b_3)\sin(f)}{pv}) - Q_D \frac{p}{r} \\ Q_L \frac{h(b_3+4\sigma_2 b_1 - 4\sigma_1 b_2)}{pv} \end{bmatrix} \tag{42}$$

With this in hand, the differential atmospheric force vector, Δa_L, which represents the difference in atmospheric forces between two spacecraft:

$$\boldsymbol{\Delta a}_L = \boldsymbol{a}_{L,D} - \boldsymbol{a}_{L,C} \tag{43}$$

Following the approach of Harris,[3] this differential aerodynamic force vector is considered with respect to a geometrically-identical chief with an attitude that is aligned with the orbit frame, i.e. the chief perturbing attitude components are set to zero. In this example, differencing the two spacecraft's aerodynamic force vectors will leave only the first-order attitude dependent terms, allowing for a linear mapping to be constructed between the MRP control vector and the aerodynamic force components in the orbit frame. The Jacobian of the differential aerodynamic forces vector with respect to a small, controlled "trim" MRP is given by

$$\frac{\partial \boldsymbol{a}_L}{\partial \boldsymbol{\sigma}} = \begin{bmatrix} \frac{\partial Q_L}{\partial \boldsymbol{\sigma}}\left(\frac{h(b_1+4\sigma_3 b_2-4\sigma_2 b_3)}{rv}\right) + Q_L \frac{\partial}{\partial \boldsymbol{\sigma}}\left(\frac{h(b_1+4\sigma_3 b_2-4\sigma_2 b_3)}{rv}\right) - \frac{\partial Q_D}{\partial \boldsymbol{\sigma}} e\sin(f) \\ \frac{\partial Q_L}{\partial \boldsymbol{\sigma}}\left(-\frac{eh(b_1+4\sigma_3 b_2-4\sigma_2 b_3)\sin(f)}{pv}\right) + Q_L \frac{\partial}{\partial \boldsymbol{\sigma}}\left(-\frac{eh(b_1+4\sigma_3 b_2-4\sigma_2 b_3)\sin(f)}{pv}\right) - \frac{\partial Q_D}{\partial \boldsymbol{\sigma}}\frac{p}{r} \\ \frac{\partial Q_L}{\partial \boldsymbol{\sigma}}\frac{h(b_3+4\sigma_2 b_1-4\sigma_1 b_2)}{pv} + Q_L \frac{\partial}{\partial \boldsymbol{\sigma}}\frac{h(b_3+4\sigma_2 b_1-4\sigma_1 b_2)}{pv} \end{bmatrix} \tag{44}$$

Under the simplifying assumption that averaged lift and drag coefficients can be used, the dominant driver of variation in the lift and drag force is due to the dependence of aerodynamic forces on the spacecraft's flow-facing projected area. Here, a linearization strategy shown to be effective for HCW-derived dynamics[3] is applied to the projected area:

$$A_p = A_i(\hat{\boldsymbol{n}}^T[TB(\boldsymbol{\sigma}_p)][BN(\boldsymbol{\sigma}_r)]^{\mathcal{N}}\hat{\boldsymbol{v}}) \tag{45}$$

Without loss of generality, the inertial velocity direction is also rotated into the chief Hill reference frame. Under the assumption of circular orbits, the inertial direction of the velocity vector in the chief reference frame is simply the $\hat{\boldsymbol{h}}_\theta$ unit vector. The per-facet projected area is therefore:

$$A_p = A_i(\hat{\boldsymbol{n}}_i^T[TB(\boldsymbol{\sigma}_p)][BH(\boldsymbol{\sigma}_r)]^{\mathcal{H}}\hat{\boldsymbol{v}}) \tag{46}$$

if that σ_p is small, second order terms can be neglected, and Equation 46:

$$A_p = A_i(\hat{\boldsymbol{n}}_i^T[BN(\boldsymbol{\sigma}_r)]\hat{\boldsymbol{v}} - 4\hat{\boldsymbol{n}}_i^T[\boldsymbol{\sigma}_p\times][BN(\boldsymbol{\sigma}_r)]\hat{\boldsymbol{v}}) \tag{47}$$

This expression contains two primary components: a constant term driven by the selected reference MRP, and a linearized rotational component based on the perturbing MRP. In the consideration of the differential lift vector, the term driven by the reference MRP is canceled by the corresponding term for the target orbit's aerodynamic forces.

LYAPUNOV CONTROL

Following the approach of Bennett,[13] linearized relative orbital elements (LROEs) are chosen as a nonsingular parameterization of relative orbital motion. While this element set does require the assumption of a circular "chief" orbit to linearize about, this assumption is reasonable in the presence of drag forces which tend to circularize orbits over time. As their name implies, these elements are constant in the Keplerian case; however, perturbation forces can affect their values, leading to the following differential equation for their evolution:

$$\dot{\boldsymbol{\alpha e}} = [B](\boldsymbol{a}_d + \boldsymbol{u}) \tag{48}$$

where $[B]$ is the matrix of sensitivities derived by Bennett, $\boldsymbol{a}_d$ is the vector of perturbing accelerations from the environment, and $\boldsymbol{u}$ is the vector of control accelerations. Using the lift-derived acceleration sensitivity matrix $[B_{\text{lift}}]$, this expression is refactored for the desired system, denoting the disturbance dynamics as $[A(\boldsymbol{oe})]$:

$$\dot{\boldsymbol{oe}} = [A(\boldsymbol{oe})] + [B][B_{\text{lift}}]\boldsymbol{\sigma} \tag{49}$$

A similar Lyapunov-based control strategy is derived to drive the LROE states to zero. Following Bennett, we select our Lyapunov function candidate to be

$$V = \frac{1}{2}\boldsymbol{oe}^T[P]\boldsymbol{oe} \tag{50}$$

whose time derivative is

$$\dot{V} = \boldsymbol{oe}^T[P]([A(\boldsymbol{oe})] + [B][B_{\text{lift}}]\boldsymbol{\sigma}) \tag{51}$$

Following 18, $\boldsymbol{\sigma}$ is chosen as

$$\boldsymbol{\sigma} = -[B_{\text{lift}}]^T[B]^T[P]\boldsymbol{oe} \tag{52}$$

Selecting this as the control law for the guided attitude yields

$$\dot{V} = \boldsymbol{oe}^T[P]([A(\boldsymbol{oe})] - [B][B_{\text{lift}}][B_{\text{lift}}]^T[B]^T[P]\boldsymbol{oe}) \tag{53}$$

$$\dot{V} = \boldsymbol{oe}^T[P]([A(\boldsymbol{oe})] - \boldsymbol{oe}^T[P][B][B_{\text{lift}}][B_{\text{lift}}]^T[B]^T[P]\boldsymbol{oe}) \tag{54}$$

As indicated by prior studies, this approach provides global Lyapunov stability when

$$[P][B][B_{\text{lift}}][B_{\text{lift}}]^T[B]^T[P] \gg \boldsymbol{oe}^T[P]([A(\boldsymbol{oe})])$$

In addition, similar arguments can readily be made for other nonsingular orbit element parameterizations, such as those used by Anderson.[17]

NUMERICAL VALIDATION

Linear System Results

To demonstrate the viability of this approach, a linear scenario based on a spacecraft maneuvering into a different along-track position and a different inclination is considered. The initial orbital elements, and the corresponding LROE states, are presented in Tables 2 and 3. Then, the control law given by Equation 52 is integrated in a closed-loop manner. The results of this simulation are shown in Figure 3(c), with corresponding commanded trim MRPs shown in Figure 3(a). This scenario is intended to show fine-tuning of an orbit with an undesirable out-of-plane component, using a cubesat-sized spacecraft.

Table 2. Chief and deputy classical orbital elements.

Orbital Element	Chief	Deputy
a	6628.137 km	6628.137 km
e	0	0
i	45.0°	45.0001 °
ω	30.0°	30.0°
Ω	20.0°	20.0°
f	20.0°	19.999°

Table 3. Linearized Relative Orbital Elements for the relative orbit specified in Table 2

LROE	Value
A_1	7.573×10^{-2} m
A_2	9.942×10^{-6} m
x_{off}	-0.101 m
y_{off}	1.988 m
B_1	7.435 m
B_1	-8.862 m

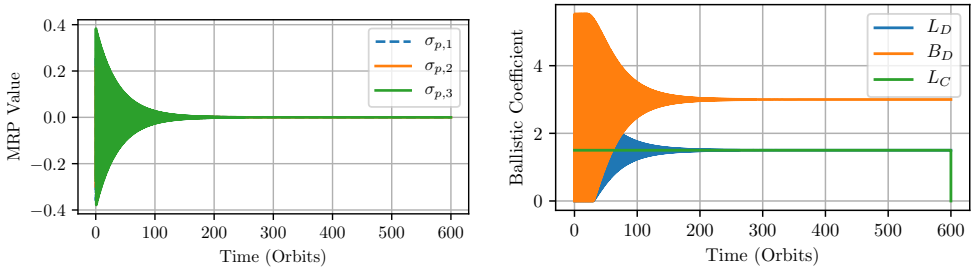

(a) Attitude Trajectory

(b) Lift and Drag coefficient trajectories

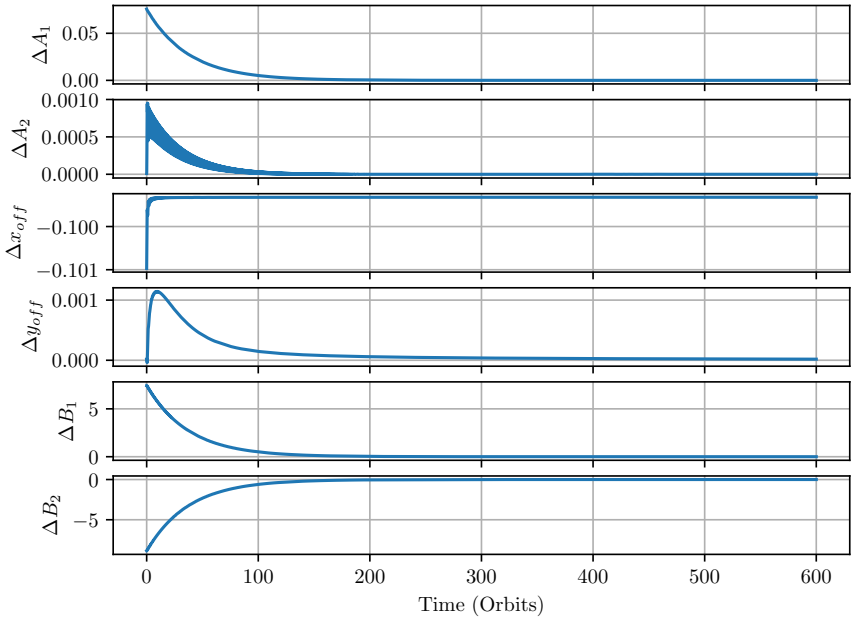

(c) States

Figure 3. Lyapunov control results for the linear system.

As shown in Figure 3, each of the LROE states is driven to zero save for the x_{off} state, which is instead stabilized. Closer examination of the patterns apparent in the lift and drag coefficient variation reveals that the lift and drag coefficients vary with one another offset by their difference in lift and drag coefficients - that is, that increasing one necessarily increases the other due to their codependence on the spacecraft's projected area. The lack of convergence implies that there is a trade-off between in-plane and out-of-plane convergence when using lift and drag for control, as prior studies have demonstrated convergence for in-plane states of cubesat-sized spacecraft within tens of orbits, rather than hundreds.

Additionally, it is notable that, while realistic attitude motion is not simulated here, the commanded MRPs are soundly within the linear regime while still achieving convergence.

Nonlinear Simulation

A major concern with this approach is the numerical magnitude of the neglected natural dynamics $[A(\boldsymbol{\alpha e})]$. To evaluate the true impact of these neglected higher-order-terms on the system, a full nonlinear simulation was run using the "truth" dynamics outlined in Section and the control strategy defined in Section . The scenario parameters are identical to those used for the linear simulation, allowing for direct comparison. The results of these simulations are shown in Figure 4.

A number of dynamics are revealed in this nonlinear simulation. First, the out of plane states decay towards zero, indicating the success of atmospheric lift in damping out out-of-plane errors over time. Errors in the in-plane position are oscillatory in nature, and do not grow; however, the size of the in-plane "error ellipse" given by A_1 and A_2 grows over time. Exploration via gain-tuning individual elements of $[P]$ has revealed a trade-off between the control of in-plane and out-of-plane states from spacecraft attitude. The cause of this is apparent when examining Figure 4(b), which shows that the ballistic (drag) coefficient and lift coefficient vary together at the same time, offset by a scalar factor. Increasing or decreasing lift forces necessarily involves increasing or decreasing drag forces, which potentially causes undesirable forcing to occur. These results suggest the use of a multi-phase control strategy, in which out-of-plane errors are damped out before in-plane ones.

CONCLUSIONS AND FUTURE WORK

Including atmospheric lift in analyses of differential-drag formation flight provides the promising benefit of out-of-orbit-plane controllability. Materials which demonstrate small accommodation coefficients can generate relatively large lift coefficients, allowing for the use of differential lift alongside differential drag as a useful constellation or formation control acceleration. A linear sensitivity matrix that directly relates spacecraft attitude, lift and drag properties to in-plane accelerations has been derived and applied to extend other Lyapunov-based formation control strategies that utilize relative orbital elements. The coupled nature of lift and drag on-orbit suggests the use of multi-phase control strategies to mitigate the coupled effects of lift and drag.

ACKNOWLEDGEMENTS

This work was supported by the Department of Defense National Defense Science and Engineering Graduate Fellowship (NDSEG) Program and the CU Smead Scholars Program.

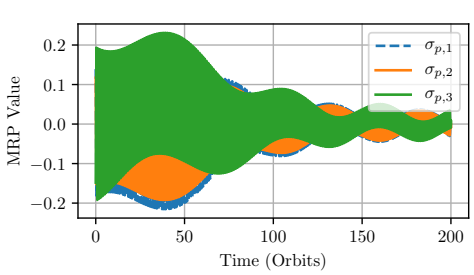

(a) Attitude Trajectory

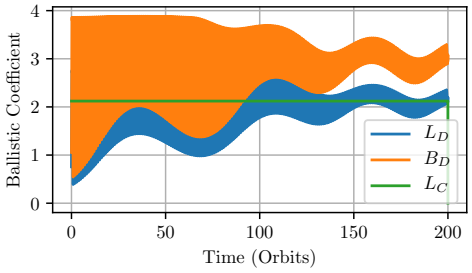

(b) Lift (L_D) and Drag (B_D)coefficient trajectories for the deputy over the simulation run.

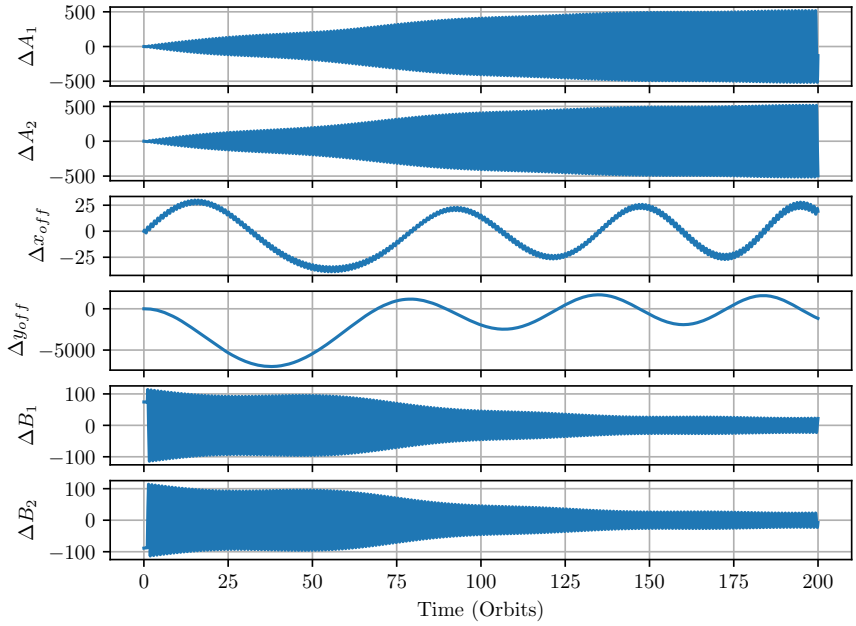

(c) States

Figure 4. Lyapunov control results for the nonlinear system.

REFERENCES

[1] D. A. Vallado, *Fundamentals of Astrodynamcs and Applications*. Space Technology Library, 4th ed., 2013.

[2] C. Foster, H. Hallam, and J. Mason, "Orbit determination and differential-drag control of Planet Labs cubesat constellations," *Advances in the Astronautical Sciences*, Vol. 156, 2016, pp. 645–657.

[3] A. T. Harris, C. Petersen, and H. Schaub, "Linear Coupled Attitude-Orbit Control Through Aerodynamic Forces," *2018 Space Flight Mechanics Meeting*, No. January, 2018, pp. 1–13, 10.2514/6.2018-0962.

[4] I. Aerospaziale, L. Sapienza, and V. Eudossiana, "Spacecraft Orbit Control using Air Drag," *56th International Astronautical Congress of the International Astronautical Federation, the International Academy of Astronautics, and the International Institute of Space Law*, 2005, pp. 1–8, 10.2514/6.IAC-05-C1.6.10.

[5] B. S. Kumar, A. Ng, K. Yoshihara, and A. De Ruiter, "Differential drag as a means of spacecraft formation control," *IEEE Transactions on Aerospace and Electronic Systems*, Vol. 47, No. 2, 2011, pp. 1125–1135, 10.1109/TAES.2011.5751247.

[6] D. Pérez and R. Bevilacqua, "Differential drag spacecraft rendezvous using an Adaptive Lyapunov Control strategy," *Advances in the Astronautical Sciences*, Vol. 145, 2012, pp. 973–991, 10.1016/j.actaastro.2012.09.005.

[7] M. Horsley, S. Nikolaev, and A. Pertica, "Small Satellite Rendezvous Using Differential Lift and Drag," *Journal of Guidance, Control, and Dynamics*, Vol. 36, No. 2, 2013, pp. 445–453, 10.2514/1.57327.

[8] L. Dellelce and G. Kerschen, "Optimal propellantless rendez-vous using differential drag," *Acta Astronautica*, Vol. 109, 2015, pp. 112–123, 10.1016/j.actaastro.2015.01.011.

[9] G. A. Bird, *Molecular Gas Dynamics and The Direct Simulation of Gas Flow*. Clarendon Press, 1994.

[10] M. D. Pilinski, "Dynamic Gas-Surface Interaction Modeling for Satellite Aerodynamic Computations," 2011.

[11] D. Hull, J. Giltner, J. Speyer, and J. Mapar, "Minimum energy-loss guidance for aero-assisted orbital plane change," *17th Fluid Dynamics, Plasma Dynamics, and Lasers Conference*, 1984, 10.2514/6.1984-1825.

[12] D. Naidu, "Orbital plane change maneuver with aerocruise," *29th Aerospace Sciences Meeting*, 1991, 10.2514/6.1991-54.

[13] T. Bennett and H. Schaub, "Continuous-time modeling and control using linearized relative orbit elements," *Advances in the Astronautical Sciences*, Vol. 156, No. 12, 2016, pp. 3613–3631, 10.2514/1.G000366.

[14] R. Krech, M. Gauthier, and G. Caledonia, "High Velocity Atomic Oxygen/Surface Accommodation Studies," *AIAA Thermophysics Conference*, No. AIAA 91-1339, 1991.

[15] E. D. Silva, "A Formulation of the Clohessy-Wiltshire Equations to Include Dynamic Atmospheric Drag," *AIAA/AAS Astrodynamics Specialist Conference*, No. August, 2008, 10.2514/6.2008-6444.

[16] O. Ben-Yaacov and P. Gurfil, "Orbital elements feedback for cluster keeping using differential drag," *Advances in the Astronautical Sciences*, Vol. 153, 2015, 10.1007/s40295-014-0022-0.

[17] P. V. Anderson and H. Schaub, "N-Impulse Formation Flying Feedback Control Using Nonsingular Element Description," *Journal of Guidance, Control, and Dynamics*, Vol. 37, No. 2, 2014, pp. 540–548, 10.2514/1.60766.

[18] H. Schaub and J. L. Junkins, *Analytical Mechanics of Space Systems*. American Institute of Aeronautics and Astronautics, 3rd ed., 2014, 10.2514/4.102400.